frontiers | Frontiers in Materials

TYPE Original Research
PUBLISHED 21 September 2022
DOI 10.3389/fmats.2022.1005387

OPEN ACCESS

EDITED BY
Feng Jiang,
University of British Columbia, Canada

REVIEWED BY
Agus Arsad,
University of Technology Malaysia, Malaysia
Ioana Chiulan,
Politehnica University of Bucharest, Romania

*CORRESPONDENCE
Naima Belhanche-Bensemra,
naima.belhaneche@g.enp.edu.dz

SPECIALTY SECTION
This article was submitted to Polymeric and Composite Materials, a section of the journal Frontiers in Materials

RECEIVED 28 July 2022
ACCEPTED 07 September 2022
PUBLISHED 21 September 2022

CITATION
Mahmoud Y, Belhanche-Bensemra N and Safidine Z (2022), Impact of microcrystalline cellulose extracted from walnut and apricots shells on the biodegradability of Poly (lactic acid). *Front. Mater.* 9:1005387. doi: 10.3389/fmats.2022.1005387

Impact of microcrystalline cellulose extracted from walnut and apricots shells on the biodegradability of Poly (lactic acid)

Yasmine Mahmoud[1], Naima Belhanche-Bensemra[1]* and Zitouni Safidine[2]

[1]Laboratoire des Sciences et Techniques de l'Environnement, Ecole Nationale Polytechnique, Alger, Algeria, [2]Laboratoire de Chimie Macromoléculaire, Ecole Militaire Polytechnique, Alger, Algeria

In this work, various microcrystalline celluloses were extracted from apricots shells (AC) and walnut shells (WC) by alkaline treatments combined with hydrogen peroxide blanching. Different composites-based poly (lactic acid) (PLA) and microcrystalline cellulose PLA/AC and PLA/WC were successfully prepared by the cast-solution method with various PLA/AC and PLA/WC ratios. PLA and prepared composites were characterized by tensile test, Fourier transform infrared spectroscopy (FTIR), melt flow index (MFI), thermo gravimetric analysis (TGA), differential scanning calorimetry (DSC) and scanning electron microscopy (SEM). Results showed an increase in Young's modulus from 802.6 MPa (PLA) to 1412.9 MPa (10% AC) and to 1145,6 MPa (7% WC) in PLA composites. A decrease in degradation temperature was recorded with increasing microcrystalline cellulose percentage in PLA composites from 354°C (PLA) to 328°C (PLA/10% AC) and 339°C (PLA/10% WC). An enhancement in crystallinity rate was observed after incorporation of the microcrystalline cellulose from 30.42% (PLA) to 37.97% (PLA/7% WC) and 38.47% (PLA/10% AC). Furthermore, the biodegradation was evaluated by a soil burial test. A loss in composites weights of 38% (PLA/7% WC), 13% (PLA/7% AC) and 14% (PLA) was obtained after 12 months within soil burial test. Finally, the presence of MCC extracted from walnut shells in PLA matrix at 7% of content exhibited the best mechanical properties, crystalline structure and biodegradability rate.

KEYWORDS

biocomposites, poly (lactic acid), microcrystalline cellulose, apricots shell, walnut shell, characterization, biodegradation

Introduction

Plastics materials are commonly used in industrial societies and their production has exponentially grown since 1950, due to their physical and chemical properties. In the same time, the rise of plastic wastes and the lack of waste management induced a rapid increase of the plastic pollution in natural environments, since they are largely non-biodegradable and persist in many environmental niches (Jambeck et al., 2015). Therefore, plastic particles (macro or micro plastics) were observed in oceans (Eriksen et al., 2014), atmosphere (Dris et al., 2016) and sediments (Van Cauwenberghe et al., 2015). These particles were accumulated in food chains through agricultural land, terrestrial, oceans and water supplies (Zhang D et al., 2020). Due to its potential harmful effects on human health and aquatic environment, the plastic pollution become a major environmental concern (Keswani et al., 2016). In particular, these plastics can contain many chemical substances and additives which are classified as toxic and dangerous to human health and the proper functioning of the food chain, which can cause several irreversible impacts (Acquavia et al., 2021). In order to deal with the negative effects of plastic pollution, the European parliament developed measures aiming to reduce the quantities of plastic wastes. As a consequence, many efforts are being made in the scientific world to find bio-based alternatives which could potentially replace them. This has led to the development of varied fields of research in bioplastics production (Cinar et al., 2020).

Bioplastics materials are obtained from renewable resources and can be biodegradable and/or compostable. Among that, Poly (lactic acid) (PLA) is one of the most promising materials to replace conventional plastics. PLA is a thermoplastic which can be synthesized by condensation of lactic acid or ring opening polymerization of lactide (Drumright et al., 2000). Lactic acid and lactide are derived from the fermentation of polysaccharide sources, essentially polysaccharide extracted from corn starch (Fortunati et al., 2010). The use of PLA in industrial societies has increased, due to high mechanical strength, easy processability and good thermal properties compared to other polymers based on fossil resources. In order to improve its properties to widen its field of application, PLA composites were developed. Among the most used fillers to enhance PLA properties reported in literature, calcium carbonate (Jiang et al., 2007), layered silicate (Zou et al., 2012), montmorillonite (Jiang et al., 2007; Ibrahim et al., 2019), graphene (Batakliev et al., 2019), carbon nanotubes (Zhou et al., 2018; Batakliev et al., 2019), chitin (Olaiya et al., 2019) and cellulosic fibers (Lu et al., 2014) can be mentioned.

Cellulose fiber is the main component of plant fibers and is considered as a biopolymer. It is usually attached to other components such as hemicellulose, lignin, pectin, lipids and waxes, all found as minor constituents (El Achaby et al., 2018). Cellulose fibers can be extracted from several agricultural wastes like wood, bamboo, flax, wheat (Chen et al., 2011), almond shell (Maaloul et al., 2017), corn stalk (Costa et al., 2015), sisal (Moran et al., 2008) etc.

The isolation of cellulose fibers requires the removal of other components and several treatments were developed to recover these constituents at different forms: microfiber cellulose (Moo-Tun et al., 2020), nanofiber cellulose (Frone et al., 2013), cellulose fiber, microcrystalline cellulose (Mahmoud et al., 2021) and nano-crystalline cellulose (El Achaby et al., 2018). The final physico-chemical properties of cellulose depend on its treatment method, the origin and the initial composition of the raw material (biomass).

The properties of PLA composites are influenced by the characteristics of cellulose fibers and their method of elaboration. The use of reinforcements that provide large surface area is considered as a good technique for obtaining better interaction between the matrix and reinforcement, leading to improved properties (Mathew et al., 2004).

The presence of microcrystalline cellulose (MCC) derived from wood pulp by acid hydrolysis used as filler for PLA showed that the mechanical and crystalline structure properties decrease for the composites compared to pure PLA. Nevertheless, its showed better biodegradation propriety, due to the poor adhesion between MCC and the PLA matrix (Mathew et al., 2004). On another side, PLA composites filled with MCC extracted from oil palm biomass prepared by casting solution showed an increase in Young's modulus and thermal stability, while the tensile strength and elongation at break for composites decreased with addition of MCC (Haafiz et al., 2013). At present MCC is commercially available in different grades and can be obtained by hydrolysis of wood and cotton using dilute mineral acids (Haafiz et al., 2013).

In the present paper, a valorization of the microcrystalline cellulose extracted from walnut shells and apricot shells (WC and AC) reported in a previous work (Mahmoud et al., 2021) was done in order to elaborate PLA composites using cast solution. To the best of our knowledge, there is no single report have been made in open literature on the use of the MCC extracted from walnut shells or apricot shells for the preparation of PLA composites. Only few studies were carried out on extraction of MCC from walnut shells (Hemmati et al., 2018; Harini and Chandra Mohan, 2020).

This study aims to evaluate the effect of the MCC presence in PLA matrix and to study the effect of MCC origin (AC or/and WC) and to optimize the MCC content in PLA matrix in order to get a best biodegradability. For that purpose, various composites PLA/AC and PLA/WC were prepared by the cast-solution method. Their mechanical, rheological, thermal, water absorption, moisture content, morphological and biodegradability properties were investigated. The ability of biodegradation for prepared biocomposites and PLA was assessed by soil burial test during 12 months.

Experimental

Materials

PLA (Nature Works 2002D) (MFI = 6.18 g/10 min, density = 1.23, Tg = 63°C, Tm = 154°C, Mw = 215,000, Mw/Mn = 1.9 and D-isomer = 4.2%) was used (Bouti et al., 2022). WC and AC microcrystalline cellulose (particle size ≤40 μm, holocellulose content was 85.0 et 87.0% and crystallinity index was 86.4 and 80.3% for WC and AC, respectively) used in this work are extracted from apricots and walnut shells according alkaline treatment and peroxide bleaching (Mahmoud et al., 2021). Chloroform (99.9%) was supplied by Biochem.

Composites preparation

Composites based PLA and microcrystalline cellulose extracted from apricots and walnut shells (Mahmoud et al., 2021) (PLA/AC and PLA/WC) were prepared by the cast-solution method. Various ratios (4, 7 and 10 wt%) of AC and WC were added in chloroform solution (50 ml) and stirred during 30 min at ambient temperature. After 30 min, PLA pellets were added to obtain a 10 wt% saturated solution. The mixture was stirred at ambient temperature for 2 h in order to obtain homogeneous solution which was immediately cast on clean glass plates (64 × 96 mm^2). Solvent was evaporated at ambient temperature. Plates of approximately 2 mm of thickness and 5 g were obtained.

Characterization methods

Fourier transform infrared spectroscopy

Attenuated total reflectance (ATR) Fourier-Transform Infrared Spectroscopy (FTIR) was used to determine changes in physical and chemical bonding and interactions on the surface of PLA and the microcrystalline cellulose WC and AC. The spectroscopic analysis of the biocomposites and the PLA was carried out using an IR Tracer-100_NIS-PC-SHIMADZU instrument type spectrometer between wave numbers of 600–4,000 cm^{-1} in transmittance mode with a resolution of 4 cm^{-1}.

Tensile testing

Tensile properties were measured using a Lloyd brand device machine. Dumbbell shape samples are cut according to DIN EN ISO 527–2 Type 5A. Five specimens were tested with a tensile speed set at 20 mm min^{-1} and finally the average value was considered. Tensile strength, Young's modulus, and elongation at break were measured.

Melt flow index

The melt flow index (MFI) of PLA and PLA composites was measured using a ZWICK®/ROELL MFLOW device under the temperature of 170 C and a load of 2.16 kg.

Moisture content

The moisture content (MC) of PLA and its composites was determined by drying three samples of each composites (19 × 12 × 2 mm^3) at 60°C until obtained constant masses. This method is inspired by the method used by Moo-Tun et al., Moo-Tun et al. (2020). The moisture content (MC) was determined according to Equation 1.

$$MC\ (\%) = \frac{W_t - W_0}{W_0} \times 100 \quad (1)$$

Where: W_t and W_0 are weight (g) of sample before and after drying, respectively.

Samples of PLA and prepared composites (19 × 12 × 2 mm^3) were dried for 24 h at 60°C and weighed to determine initial weight. According to the "ASTM D 570" standard, the samples were immersed in a container of distilled water at room temperature. They were removed water, at different time intervals, carefully wiped with paper, and then the weight was measured. A KERN analytical balance with 0.0001-g precision was used. The water absorption rate was calculated according to Equation 2.

Water absorption

Samples of PLA and prepared composites (19 × 12 × 2 mm^3) were dried for 24 h at 60°C and weighed to determine initial weight. According to the "ASTM D 570" standard, the samples were immersed in a container of distilled water at room temperature. After a time of immersion, the samples are taken out from the water, wiped with paper to eliminate the excess of water not absorbed, then the weight was measured. A KERN analytical balance with 0.0001-g precision was used. The water absorption rate was calculated according to Equation 2.

$$WA\ (\%) = \frac{W_{t1} - W_0}{W_0} \quad (2)$$

Where W_o and W_{t1} are the weight (g) of the sample before and after immersion time (h).

Thermogravimetric analysis

The thermal stability of the PLA and the composites (PLA/AC and PLA/WC) was evaluated using SETARAM Labsys Evo-gas instrument under dynamic nitrogen flow of 40 $ml.min^{-1}$ from 40 to 600 C at a heating rate of 10 $C.min^{-1}$. The weights of samples were approximately 25 mg.

Differential scanning calorimetry

The study of the crystallization behavior of the samples was carried out using a differential scanning calorimeter (DSC131 Evo) under nitrogen flow 50 ml min^{-1}. The samples were first heated up from 40 to 200°C (first heating cycle). Then, they were cooled down from 200 to 40°C (cooling cycle) and finally they were heated up again from 40 to 200°C (second heating cycle). The heating and cooling rates were maintained at 10°C.min^{-1} in all the different cycles. The enthalpies of fusion and crystallization of PLA and its composites were calculated from the DSC curves by integrating the appropriate peaks. Then the degree of crystallinity (X_c, %) of the different biocomposites was calculated using Equation 3 (Dong et al., 2014).

$$X_c\,(\%) = \frac{\Delta H_m}{\Delta H_m^0} \times \frac{100\%}{W_1} \tag{3}$$

Where ΔH_m is the heat of fusion of the composites, ΔH_m^0 is the heat of fusion of 100% crystalline PLA (ΔH_m^0 = 93.7J.g − 1) and W_1 is the weight fraction of PLA in the composite.

Optical and scanning electron microscopy

To test PLA/microcrystalline cellulose adhesion and composites morphology varied with the variation of microcrystalline cellulose content, scanning electron microscopy (SEM) and optical microscopy (OM) investigations were undertaken.

Microscopic photographs for PLA and composites-based PLA/AC and PLA/WC were observed using a Zeiss Axioskop coupled with an Optimas 1.5 picture analysis system. The magnification was 100×.

The surface morphologies of samples (PLA, PLA +4% AC, PLA +7% AC and PLA +10% AC) were investigated via a JEOL® JSM-6360 model using different magnification for PLA and its composites-based AC microcrystalline cellulose, in order to observe the surface adhesion between PLA and AC. The variation of the surface of composite with the variation of microcrystalline cellulose content was investigated.

Soil burial degradation test

The biodegradation process was carried out under barn soil humidity and natural climate at an interior temperature close which is around 25°C for a period of 12 months. For each formulation 3 samples (19 × 12 × 2 mm^3) were buried in 100 g of soil, approximately at 2 cm deep. The samples were carefully removed from the soil, washed with distilled water and dried for 24 h at 40 C. The evolution of the mass loss of the samples was followed as a function of time.

Weight loss measurements

Weight measurements were performed by using an analytical balance with 0.0001 g precision before and after soil burial degradation testing. The weight loss (WL) of the samples was estimated according to Equation 4 (Lv et al., 2017).

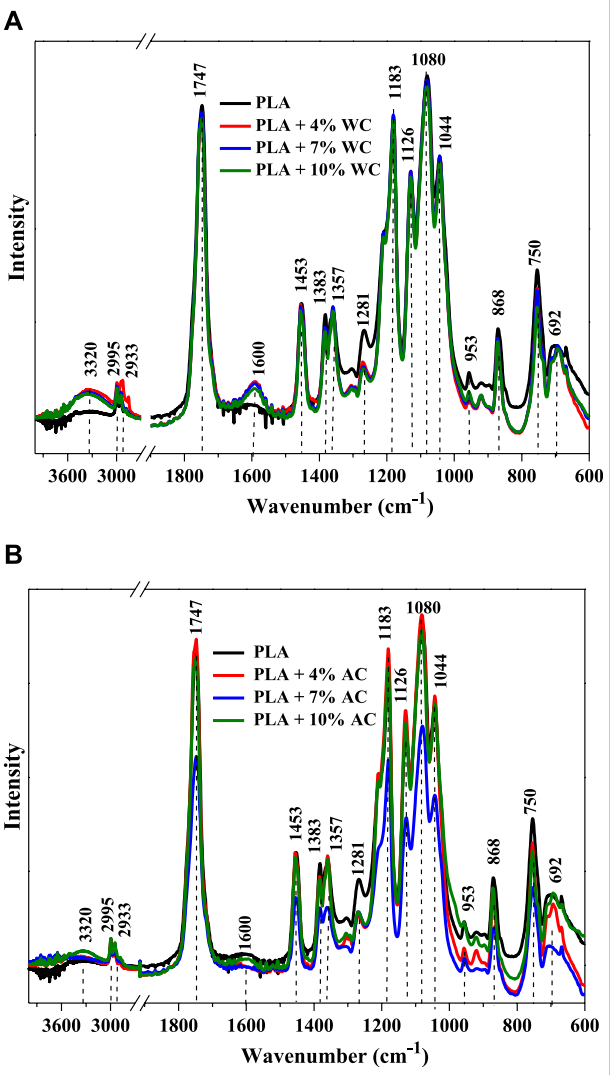

FIGURE 1
FTIR-ATR spectra of: **(A)** PLA and composites PLA/WC at different ratios (4, 7 and 10%); **(B)** PLA and composites PLA/AC at different ratios (4, 7 and 10%).

$$WL\,(\%) = \frac{W_0 - W_{t2}}{W_0} \times 100 \tag{4}$$

Where W_0 was the initial dry weight before degradation; W_{t2} was the residual dry mass after accelerated weathering or after soil burial degradation testing at an exposure time t. An average of at least three measurements was calculated after soil burial degradation.

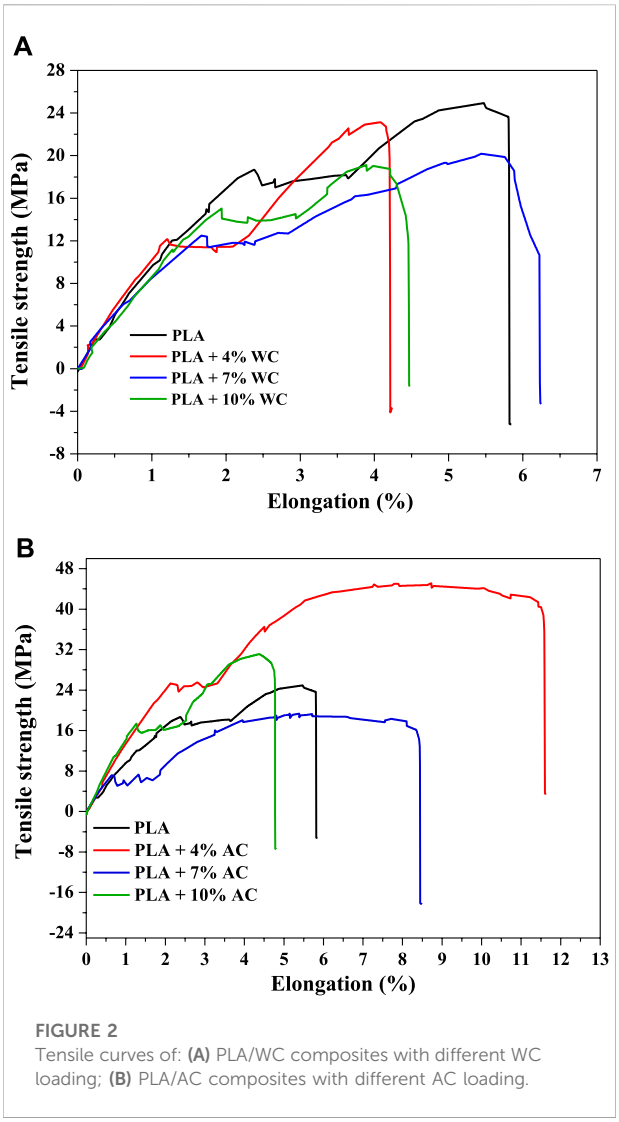

FIGURE 2
Tensile curves of: **(A)** PLA/WC composites with different WC loading; **(B)** PLA/AC composites with different AC loading.

Results and Discussion

ATR-FTIR spectroscopy analysis

ATR-FTIR spectra of PLA and its composites reinforced with microcrystalline celluloses extracted from walnut shells (WC) and apricot shells (AC) are shown in Figures 1A,B, respectively.

PLA has same characteristic IR bands observed in literature (Kaynak and Meyva, 2014; Dogu and Kaynak, 2016). The bands located at 1183, 1126 and 1080 cm^{-1} are attributed to C-O stretching vibrations (Gazzotti et al., 2019) while those situated at 1281 and 1747 cm^{-1} are attributed to bending and stretching vibrations of C=O bonds, respectively (Qu et al., 2010). The bands located at 2,995 and 2,933 cm^{-1} represent the asymmetric and symmetric stretching of C-H vibrations, and the bands located at 1383 and 1453 cm^{-1} are characteristic of symmetric and asymmetric bending of C-H vibrations, respectively (Mahmoud et al., 2018; Gazzotti et al., 2019). Low band intensity observed at 1200 cm^{-1} was attributed to the C-O-C bands and those at 868 and 953 cm^{-1} were attributed to C-C band stretching vibrations (Heidarian et al., 2017; Gazzotti et al., 2019). The bands at 1044 cm^{-1} and 3,320 cm^{-1} represent bending and stretching vibrations of–OH groups, respectively (Mofokeng et al., 2012).

The prepared composites present the same characteristic bands of PLA, with just a new small band located between 1560 and 1640 cm^{-1}, particularly for the composite PLA/WC. This band is probably due to the O-H bending of the water adsorbed by the microcrystalline cellulose (Mofokeng et al., 2012; Wang et al., 2020). This can be explained by the nonappearance of chemical interactions between PLA and the microcrystalline cellulose, but the presence of only physical interactions. Moreover, the addition of microcrystalline cellulose influences slightly the location and the intensity of the characteristic bands of PLA, in particular C=O, C-O and–OH groups. This is probably due to physical interactions and hydrogen bonds formed between the microcrystalline cellulose and PLA matrices (Yew et al., 2005; Mofokeng et al., 2012). The same observation was reported in the case of PLA/montmorillonite composites (Arjmandi et al., 2015).

Tensile properties analysis

The tensile properties of PLA and composites were determined by the stress-strain curves shown in Figures 2A,B for the composites PLA/WC and PLA/AC, respectively. The mechanical properties of composites are affected by the nature, the content, as well as interactions between the polymer matrix and the cellulosic filler (Patel et al., 2019). The mechanical characteristics of PLA and elaborated composites are given in Table 1.

The tensile test showed a considerable modification of the mechanical properties of PLA after incorporation of microcrystalline cellulose for most of the biocomposites. These changes are owed to the interactions between the polymeric matrix (PLA) and the microcrystalline cellulose (AC, WC), which apparent themselves in the form of hydrogen bonds (Patel et al., 2019).

Young's modulus and tensile stress at break of the composites increased with the increase of AC content (Table 1). Young's modulus of composites loaded with WC reached a maximum value for the composite loaded with 7%, while tensile stress at break reached a maximum value for the composite loaded with 4% WC. The increase of Young's modulus after added load was observed by several researchers (Mathew et al., 2004; Patel et al., 2019).

On the other hand, elongation at break increased after adding AC and decreased with the increase of the load, but elongation at break of the composites loaded by WC takes a maximum value

10.3389/fmats.2022.1005387

TABLE 1 Mechanical properties of the prepared composites.

Sample	Young's modulus (MPa)	Elongation at break (%)	Tensile stress at break (MPa)
PLA	802.64 ± 150.00	5.8 ± 1.0	5.5 ± 1.0
PLA + 4% WC	760.6 ± 172.56	4.2 ± 0.6	10.8 ± 0.4
PLA + 7% WC	1145.6 ± 86.09	6.2 ± 0.5	5.5 ± 0.4
PLA + 10% WC	793.22 ± 145.80	4.4 ± 0.5	6.4 ± 0.3
PLA + 4% AC	1218.58 ± 59.09	11.5 ± 0.9	13.4 ± 0.5
PLA + 7% AC	1173.42 ± 96.90	8.4 ± 0.4	11.4 ± 0.7
PLA + 10% AC	1412.88 ± 100.04	4.7 ± 1.1	12.4 ± 0.5

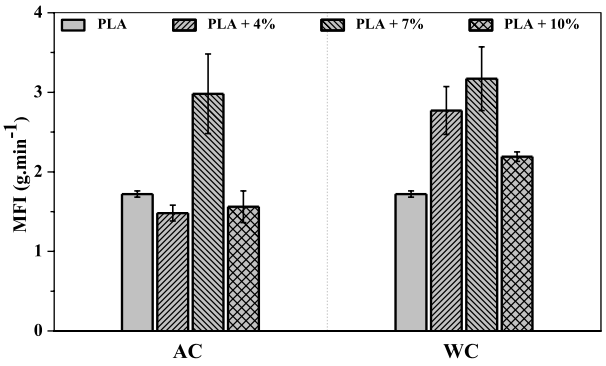

FIGURE 3
Melt flow index values of PLA and composites.

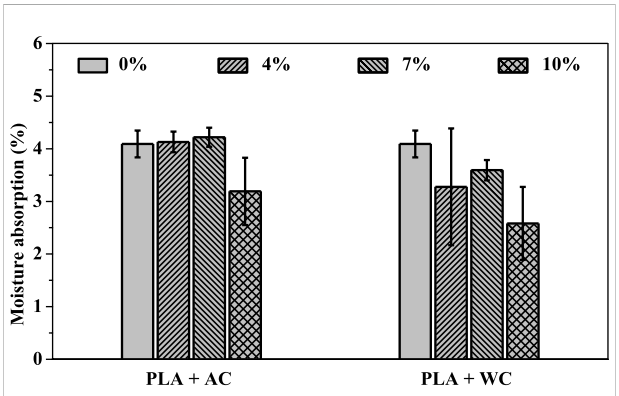

FIGURE 4
Moisture absorption analysis of PLA and prepared biocomposites.

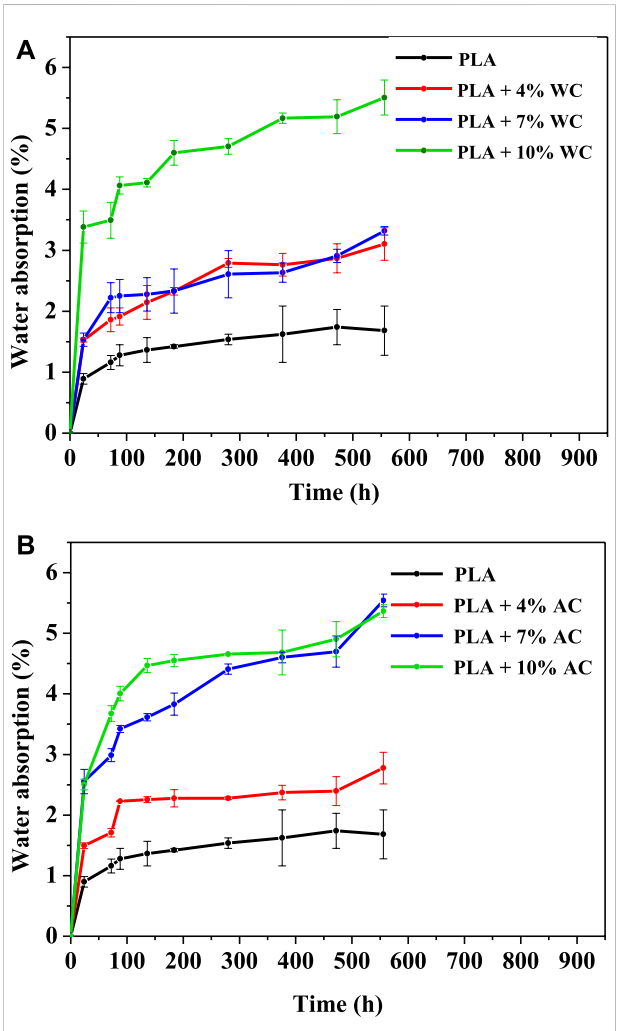

FIGURE 5
Water absorption behavior of: **(A)** PLA and PLA/WC composites; **(B)** PLA and PLA/AC composites.

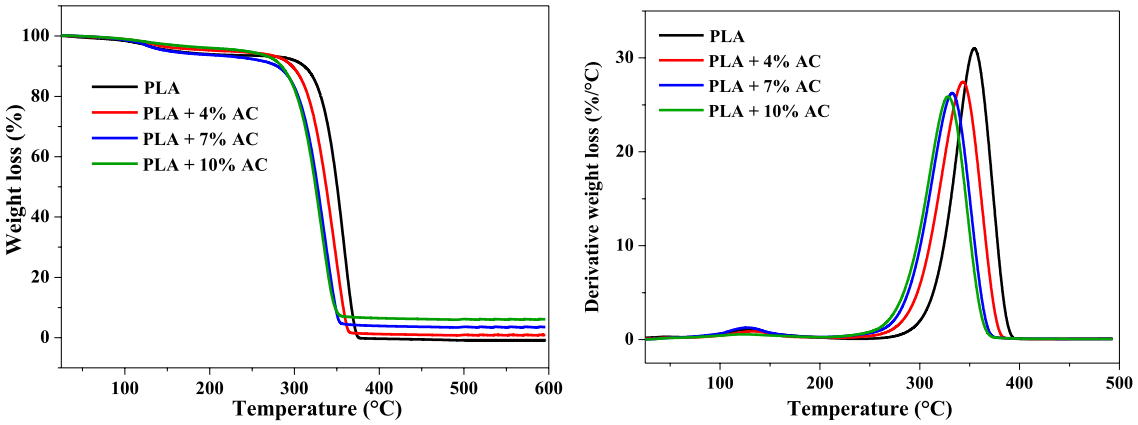

FIGURE 6
TG, and DTG curves of PLA and PLA/AC composites.

for the composite loaded at 7% while the other values (4 and 10% WC) remained lower than that of PLA.

Melt flow index measurements

The Melt flow index is an important parameter in polymer composites characterizations, Because it give information's about the variation of extrusion throughput at industrial scale (Barczewski and Mysiukiewicz, 2018), the mechanical properties and then the promising applications (Kim et al., 2014).

The effect of MCC charge for both AC and WC on PLA melt flow index (MFI) variation is presented in Figure 3. It seems that the presence of MCC in PLA increase the MFI values for all WC and AC tested content which can be attributed to the reduction in the polymer's molecular length, and then more PLA composite flow with a shorter length (Baimark and Srihanam, 2015). The slight and negligible decrease in PLA-AC composite (4% of charge) MFI can be due to the experimental and analysis errors.

The increase of MCC charge in the first stage (from 4 to 7%) enhanced the PLA composites MFI from 1.80 to 3.75 g min $^{-1}$ and from 3.47 to 3.97 g min $^{-1}$ for AC and WC, respectively. This can be explained by the fact that a poor interaction between PLA-AC or PLA-WC than PLA-PLA was created in composites. Similar behavior was reported in Kenaf fiber reinforced Floreon composites (Lee et al., 2016).

In the second stage, a farther increase in MCC charge more than 7% caused a decrease in PLA composites MFI. According to Jaafar et al., this behavior is due to the strong molecular interaction between MCC molecules (Nurul and Mariatti, 2018). Similar results were reported in Polypropylene composites reinforced with treated and non-treated flax fiber (Soleimani and Tabil, 2008).

Moisture absorption analysis of biocomposites

The sensitivity of materials to moisture is one of the parameters that negatively influences their mechanical properties, therefore limiting their applications. This sensitivity is linked to the presence of hydroxyl groups which interact with water molecules and establish strong hydrogen bonds. The incorporation of cellulose powder into the PLA polymer matrix makes it possible to establish interactions between the hydroxyl groups of cellulose and the C=O groups of PLA to form strong bonds between the two components, which makes it possible to reduce the hydrophilic behavior of the material. To verify this, the rate of moisture absorption for the different samples was evaluated and presented in Figure 4. According to this figure, the addition of microcrystalline cellulose reduced slightly the moisture content in the matrix (Heidarian et al., 2017). These results agree well with those obtained during the characterization by FTIR spectroscopy where the bands showing the hydrophilic nature of the material were more intense for the composites based on microcrystalline cellulose (AC and WC).

Water absorption

Figure 5A,B show the water absorption curves for PLA and all prepared composites (PLA/AC and PLA/WC) for 560 h. All samples exhibited a rapid water uptake at the initial stage, and later a saturation level was attained with a further increase in water absorption for all composites.

According to the shape of the curves presented in Figure 5A,B, the absorption increased rapidly during the first hours to reach equilibrium after 140 h and the further increase

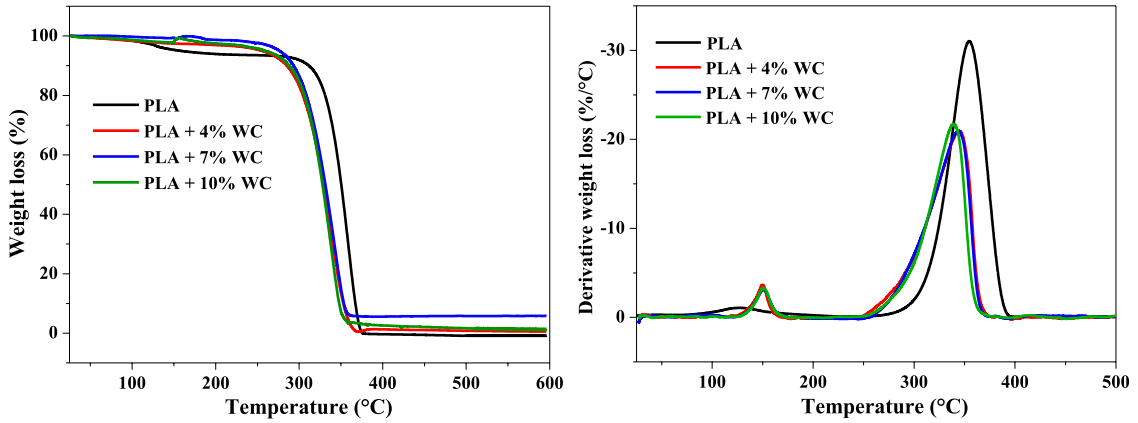

FIGURE 7
TG and DTG curves of PLA and PLA/WC composites.

TABLE 2 Thermogravimetric data of PLA and reinforced composites by AC and WC at different rates.

Composites	Moisture (%)	T_m (°C)	Ask (%)
PLA	7	375	0
PLA + 4% AC	4	365	2
PLA + 7% AC	7	354	4
PLA + 10% AC	4	351	7
PLA + 4% WC	3	371	2
PLA + 7% WC	1	356	6
PLA + 10% WC	1	356	2

was observed after 470 h. The water absorption capacity for composites increased significantly with increasing filler rate. PLA has an absorption rate of 1.5% of its initial weight. The rate of water absorption increased considerably with the increase in the rate of microcrystalline celluloses AC and WC, this rate of absorption reached its maximum capacity which is 5.5% for a charge rate of 10%. This increase is probably due to the hydrophilic nature of the filler which is greater for microcrystalline cellulose since it is richer in cellulose. Similar results were found in literature, where the absorption rate increases with increasing loading rate (Moo-Tun et al., 2020; Salim et al., 2020; Yorseng et al., 2020).

Thermogravimetric analysis

The TGA and DTG data for PLA and prepared composites are shown in Figure 6 and Figure 7 for PLA/AC and PLA/WC, respectively. All the TGA curves showed two main degradation regions. One is reportedly due to the moisture evaporation present in composites, and the other higher temperature one is attributed to depolymerization of PLA (Lee et al., 2009). The parameters such as moisture contain, ash contain after degradation and maximum degradation temperature (T_m) obtained from the TGA and DTG thermograms are given in Table 2.

TGA confirmed that the moisture contains in prepared composite decreased after incorporation of microcrystalline cellulose compared to PLA. Nevertheless, the results obtained by TGA were found to be weaker than those obtained using the method inspired by Moo-Tun et al., Moo-Tun et al. (2020). The reported data show that the thermal decomposition of PLA occurred at 375 C. The degradation temperature decreased after incorporation of microcrystalline cellulose and this temperature decreased with the increase of loading rate. According to DTG, the degradation temperature for composites loaded with 4, 7 and 10% AC decreased by 11, 22 and 26°C, respectively and composites loaded with 4, 7 and 10% WC decreased by 9, 9 and 15°C, respectively. These results indicates that the introduction of microcrystalline cellulose reduces considerably the thermal stability of PLA composites and many research confirm these results (Lee et al., 2009; Fortunati et al., 2010; Shih and Huang, 2011). Nevertheless, the thermal stability of PLA composite can also increase after treating kenaf fibers with silane (Lee et al., 2009).

The ash content for the composites reinforced by microcrystalline cellulose (AC and WC) increased compared to PLA (Table 2). This ash content is 2, 4 and 7% for composites loaded with 4, 7 and 10% AC and it is 2, 6 and 2% for composites loaded with 4, 7 and 10% WC, respectively. In summary, the incorporation of microcrystalline cellulose (AC and WC) fillers decreased the thermal stability of composites, but increased their residual ash content (Lee et al., 2009).

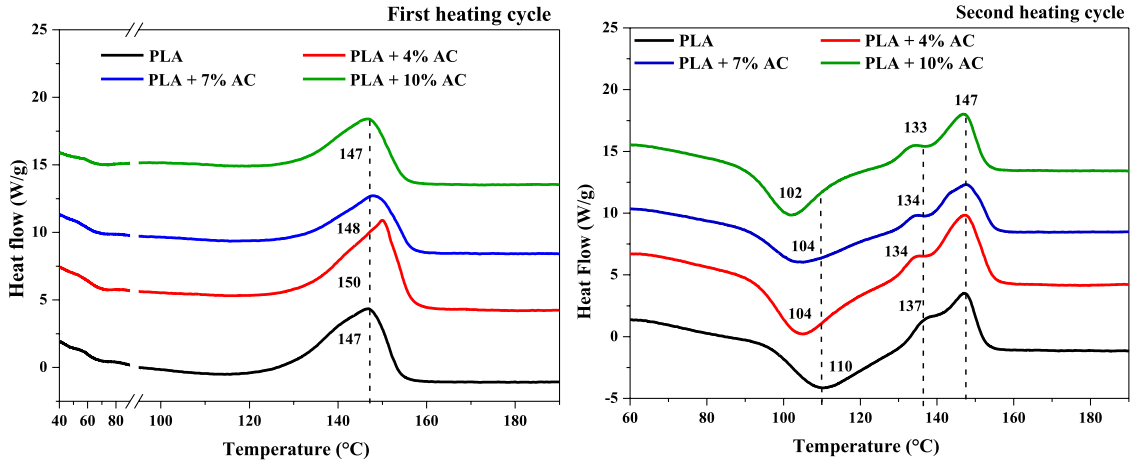

FIGURE 8
DSC thermograms for PLA and PLA/AC composites during the first and second heating.

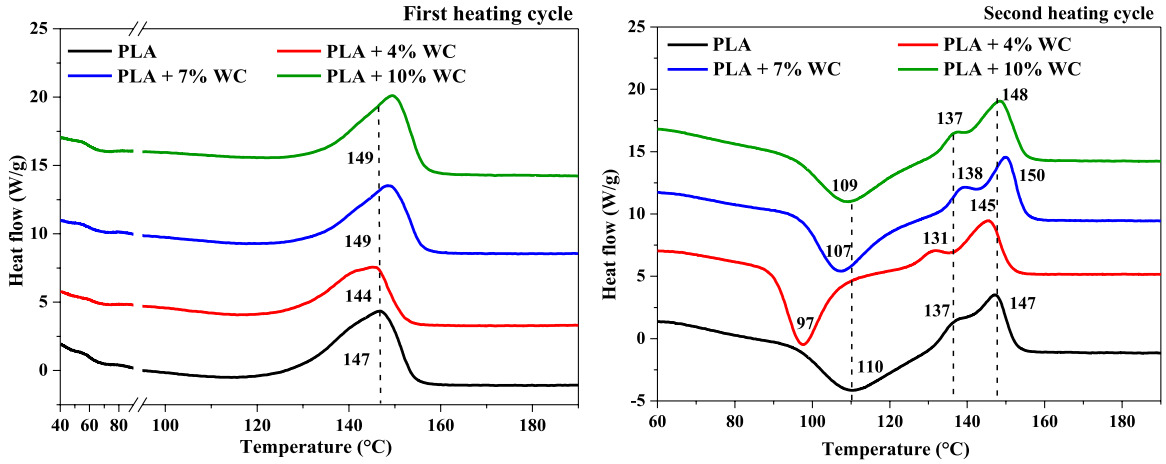

FIGURE 9
DSC thermograms for PLA and PLA/AC composites during the first and second heating.

Differential scanning calorimetry analysis

DSC analysis was performed to study the effect of filler incorporation on the thermal properties of biocomposites. DSC thermograms of PLA and PLA composites reinforced with microcrystalline cellulose (AC and WC) at different loading rates are shown in Figure 8 and Figure 9, respectively.

The thermal properties of PLA, PLA/AC and PLA/WC composites obtained during the first and second heating cycles of the DSC analysis as the glass transition temperature T_g, cold crystallization temperature T_c, melting temperature T_m, fusion processes enthalpy ΔH_m and crystallinity degree X_c are given in Table 3.

According to the obtained thermograms, it can be seen that the addition of the MCC (AC and WC) in PLA matrix did not lead to significant changes in T_g value (62.5 C) for most prepared composites. This result is similar to those reported by other researchers (Shih and Huang, 2011; Wang et al., 2020; Zhang Q et al., 2020). Nevertheless, a slight increase in T_g value was observed for PLA +4% WC. This increase can be explained by the restriction of the mobility of the polymer chains due to the interactions and bonds formed with the MCC (Shih and Huang, 2011). During the second heating cycle, the T_g could not be observed. The same

10.3389/fmats.2022.1005387

TABLE 3 Thermal properties of PLA, PLA/AC and PLA/WC composites.

	First heating cycle				Second heating cycle				
	T_g (°C)	T_m (°C)	ΔH_m (J/g)	X_C (%)	T_c (°C)	T_{m1} (°C)	T_{m2} (°C)	ΔH_m (J/g)	X_C (%)
PLA	62.5	147	38,028	40.58	110	137	147	28,511	30.42
PLA + 4% AC	62.5	150	33,963	37.76	104	134	147	31,255	34.75
PLA + 7% AC	62.4	148	33,166	38.06	104	134	147	28,388	32.58
PLA + 10% AC	62.5	146	31,895	37.82	102	133	147	32.44	38.47
PLA + 4% WC	63.5	144	31,230	34.72	97	131	145	31,430	34.94
PLA + 7% WC	62.5	149	35,204	40.40	107	138	150	33,093	37.97
PLA + 10% WC	62.5	149	31,484	37.33	109	137	148	27,962	33.16

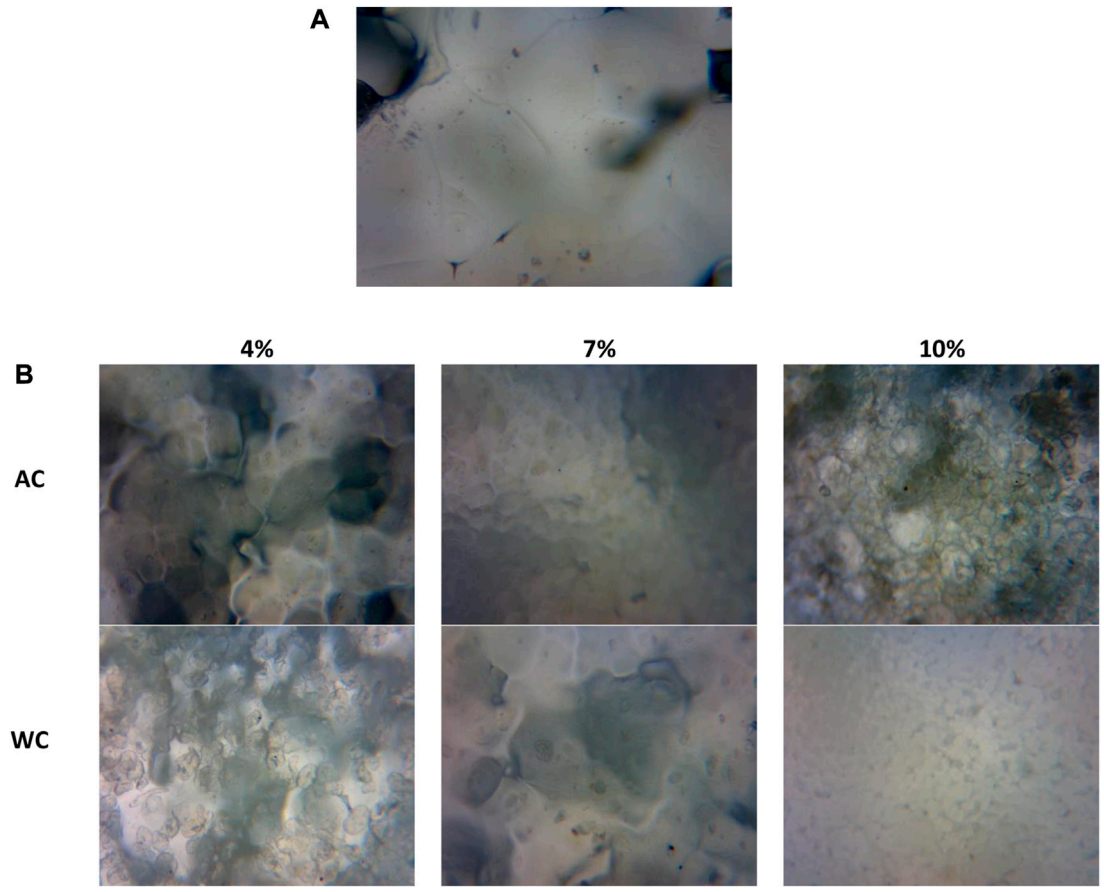

FIGURE 10
Optical images of: **(A)** PLA and **(B)** PLA composites loaded with WC and AC.

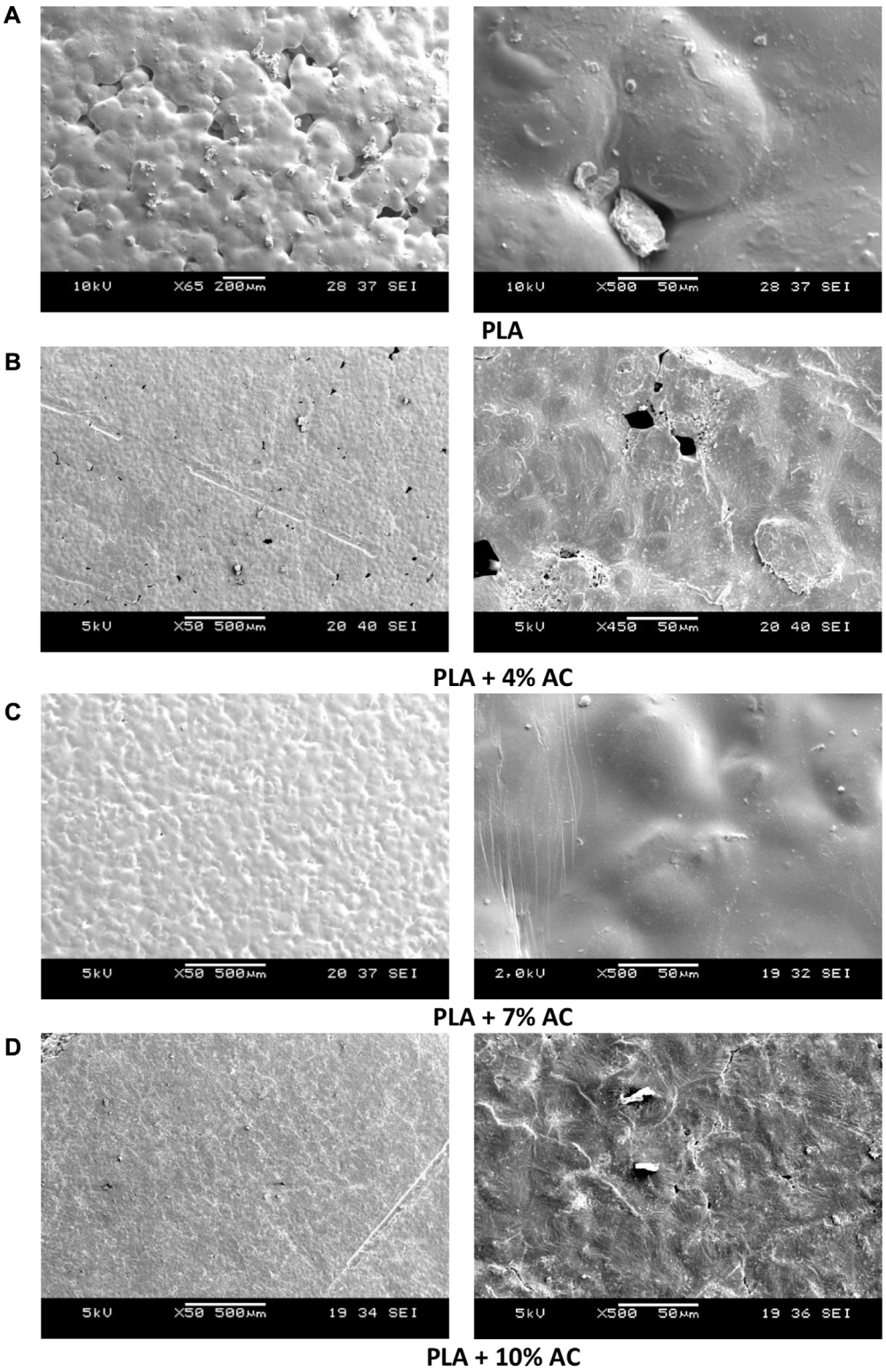

FIGURE 11
SEM micrographs of **(A)** PLA, **(B)** PLA+ 4% AC, **(C)** PLA +7% AC and **(D)** PLA +10% AC composite at different magnification.

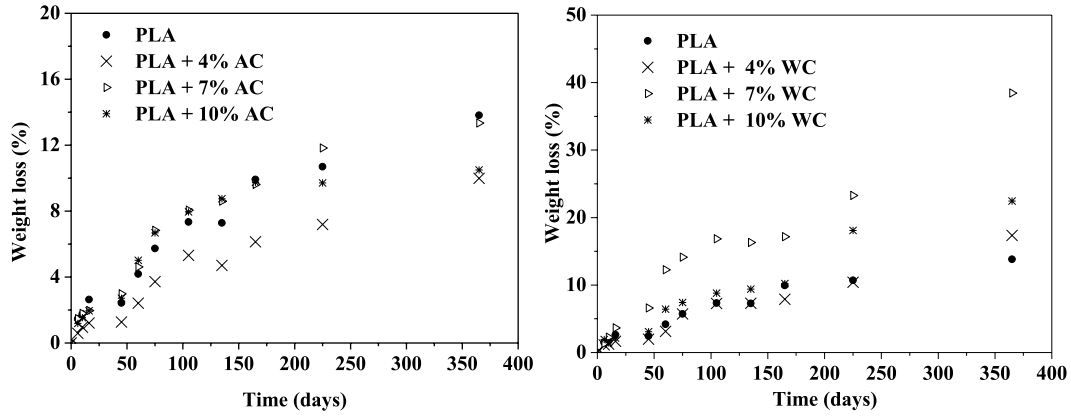

FIGURE 12
Weight losses of PLA, PLA/AC and PLA/WC composites during the soil burial test.

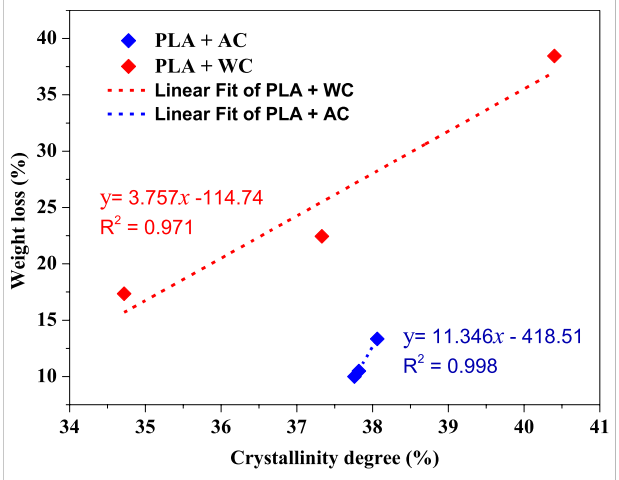

FIGURE 13
Correlation between crystallinity degree and weight loss after 1 year of soil burial test.

phenomenon was reported, accompanied with absence of cold crystallization phenomenon and was explained by strong crystallization of the composite after the previous cooling (Frone et al., 2013). This phenomenon can also be explained by the move of the T_g to lower temperatures.

In addition, the crystallization temperature T_C appears only in the second heating cycle for PLA and its composites, it decreases after incorporation of AC and WC in PLA matrices. This phenomenon has also been observed for PLA/montmorillonite biocomposites (Arjmandi et al., 2015), for PLA/microcrystalline cellulose (MCC) biocomposites (Zhang Q et al., 2020) and for composites based on high density polyethylene/rice fiber (Zhang et al., 2018). This decrease in T_c indicates that crystallization is faster and earlier for prepared composites than for PLA. According to Wang et al., the increase in crystallization temperature indicates that the filler acted as a nucleating agent (Wang et al., 2020).

The values of T_m obtained during the first heating for the composites loaded with 4, 7 and 10% WC are 144, 149 and 149 C and those loaded with 4, 7 and 10% AC are 150, 148, 146°C, respectively. These melting temperatures are mostly higher than that of PLA (147 C) except for composites filled with 4% WC and 10% AC. During the second heating cycle, the appearance of a double melting peak around 137 and 147 C was noticed. The multiple melting of PLA and prepared composites could be explained by the appearance of two types of crystallites after the previous cooling effected after the first heating cycle. The melting peak at higher temperature (T_{m2}) could be attributed to the melting of the most perfect crystal structure of PLA and the first peak located at lower temperature (T_{m1}) is attributed to the melting of the less crystal structure (Frone et al., 2013). This phenomenon of multiple fusion has been observed by several researchers (Frone et al., 2013; Wang et al., 2020).

After incorporation of MCC in the PLA matrix, the first melting temperature observed during the second melting decreased to lower temperature, except for PLA +7% WC composite, this indicates that the crystal structure changed from a less perfect structure to a more perfect structure after MCC introduction. The second melting temperature observed during the second melt is not affected for all composites charged with AC, contrary to the composite charged with WC, where a slight increase was observed, except for the composite loaded with 4% WC. According to Zhang et al., the decrease in T_g and T_m of the composites compared to that of PLA is probably due to the bad interactions caused by the free volume formed by the addition of the load and their increase indicates the improvement of the thermal stability of the composites (Zhang Q et al., 2020). During the first heating cycle, all samples showed a decrease in

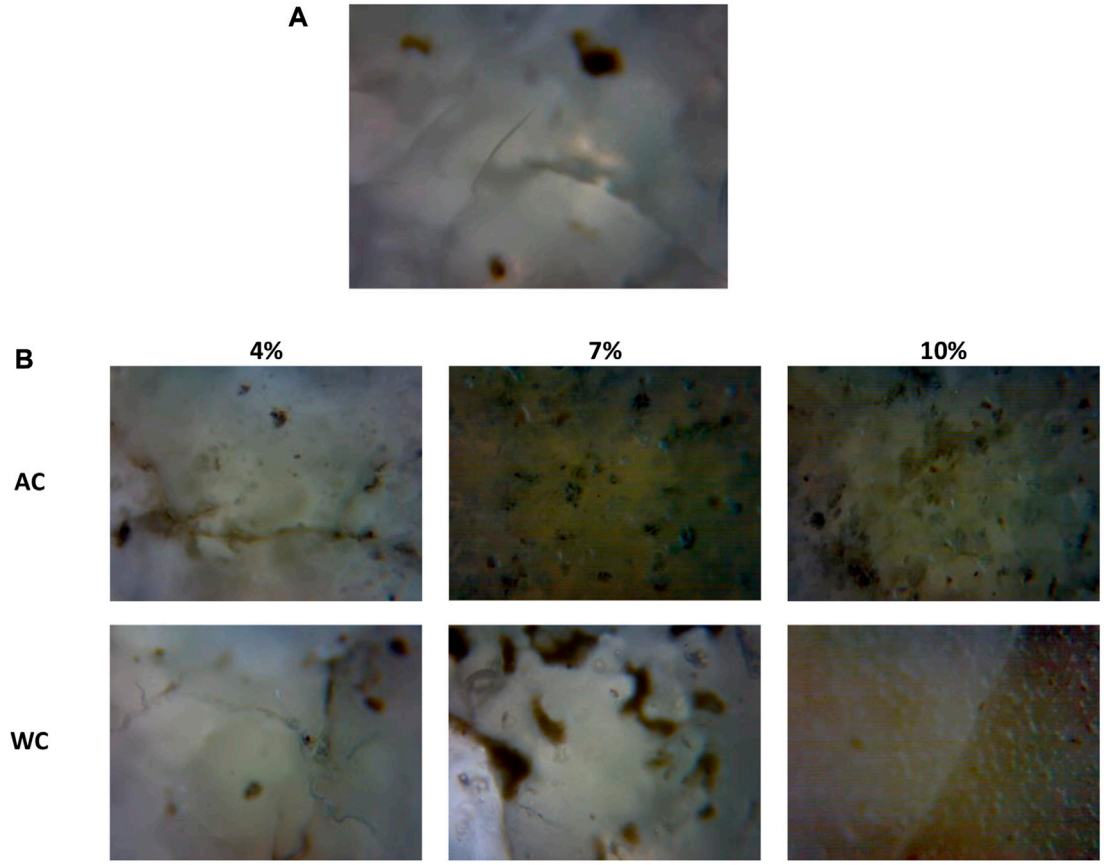

FIGURE 14
Optical images of: **(A)** PLA and **(B)** PLA composites loaded with AC and WC after 5 months of burial time with (100×) magnification.

the fusion processes enthalpy, which entails a decrease in the crystallinity degree X_c after incorporation of MMC. Nevertheless, most composites show an increase in ΔH_m compared to PLA during the second heating. This increase indicates an increase in the crystallinity degree. The increase in ΔH_m indicates that the fusion processes requires more energy (Sukyai et al., 2012).

Optical and scanning electron microscopy

To give a clearer view of surface modification of PLA and PLA composites after incorporation of CMM at different load rates (4, 7 and 10%), surfaces were characterized by optical microscopy with a magnification of (100×). Figure 10A,B show, respectively, the images of PLA surface and the effect of adding WC and AC fillers with different load rates (4, 7 and 10%) on the state of their surfaces.

Figure 10A shows that PLA presents a homogeneous and smooth surface with the presence of some air bubbles, a same observation was reported by Bouti et al., Bouti et al. (2022). Figure 10B shows the good distribution of the MCC (WC and AC) in the polymer matrix and the disappearance of air bubbles found in pure PLA.

The SEM micrographs of PLA, PLA +4% AC, PLA +7% AC and PLA +10% AC composites (Figure 11) shows a large modification in surface morphological. We can clearly see, a presence of large holes in the surface of PLA in high density. The density of this holes decreases after incorporation of microcrystalline cellulose and this density is weaker for PLA +7% AC.

As we can clearly see, the addition of 7% AC microcrystalline cellulose shows a good adhesion and compatibility between PLA and AC, the morphological surface of this composite does not show any fractures, unlike composites filled with 4 and at 10% AC. The surface fracture observed for the composites filled with 4 and 10% AC, indicating poor interfacial interaction between PLA and MCC (Arteaga-Ballesteros et al., 2021; Paul et al., 2021).

Soil burial testing

The biodegradability test of the samples was carried out without any composting and enzymatic material, but by a

simple test of burial in the ground under normal environmental conditions. The evolution of the weight loss as a function of burial time in the ground for the composites loaded by 4, 7 and 10% (AC and WC) is shown in Figure 12. All samples showed an increase in weight loss with increasing burial time. PLA shows a weight loss percentage of 4.20, 8.50 and 13.80% after 2, 5 and 12 months of burial time, respectively. Similar results were found, where the degradation of PLA under normal conditions is estimated by 5% after 3 months of burial time (Ramesh et al., 2021).

After 12 months of burial in the soil, the composites loaded with MCC showed considerable weight loss, in particular for the composites loaded with WC. Composites loaded with 4, 7 and 10% WC showed 17.35, 38.44 and 22.44% weight losses after 12 months' burial time, respectively. The composites loaded with 7% WC show a greatest weight loss which reached 38.44% after 12 months of burial, this is explained by the good distribution of WC within the PLA matrix, according to many research, the addition of cellulose in the PLA matrix increases the degradation rate (Yussuf et al., 2010; Ramesh et al., 2021; Yussuf et al., 2010; Yussuf et al., 2010). Composites reinforced with 18% of treated coconut fibers show more degradation rate than PLA, the weight loss is estimated at 34.9% after 18 days of burial time, due to of the hydrophilic nature of coconut fibers (Dong et al., 2014).

Composites loaded with 4, 7 and 10% AC rates show 10.00, 13.37 and 10.49% weight losses after 12 months' burial time, respectively. The composites loaded with AC showed a weight loss that are not considerably modified compared to pure PLA and the composite loaded with 7% AC show also a maximum weight loss which is explained by a good distribution within the PLA matrix.

The obtained results from soil burial test, the presence of MCC in PLA composite structure enhance the biodegradability rate of PLA in the most tested MCC content, where the optimum biodegradation rate was recorded with 7% for both AC an WC content in PLA. From another hand, it is important to signal that PLA is known as a biodegradable polymer with eco-friendly bioproduct (CO_2 and H_2O) as reported by silva et al. Silva et al. (2020). Furthermore, Kumar et al., reported a decrease in time needed for the mineralization of 90% of PLA carbon from 60 ± 2 days for PLA with 5% of charge (deoiled algae biomass) to 95 ± 7 days for pristine PLA (Kumar et al., 2021).

In order to better understand the behavior of the materials produced, we tried to find a relationship between the rate of crystallinity of the material and its capacity for this degradation in the soil. The exploitation of these results made it possible to plot Figure 13.

According to Figure 13, there is a proportional relationship between crystallinity degree of the composite and its ability to degrade after soil burial. This relationship is linear for the two composites elaborated. Similar relationships have been found for other composites elaborated as PLA/chitosan (Yaacob et al., 2016), PLA/microcrystalline cellulose deoiled algae biomass and PLA/amorphous cellulose (Hafizi et al., 2020).

Optical microscopy analysis

Figure 14A,B) show, respectively, optical images of PLA and PLA composites reinforced with WC and AC, after 5 months of soil burial. Before soil burial, PLA and composites reinforced with AC and WC (Figures 10A,B) had a relatively smooth and clear surface. After 5 months of burying, PLA and composites reinforced by AC and WC showed erosion of the surface, the appearance of black spots and cracks manifested on the surface indicating the degradation of the samples. Similar observations were made by Alimuzzaman et al. on PLA and its composites after 120 days' of burial in compost condition, using scanning electron microscope (Alimuzzaman et al., 2014).

Conclusion

Microcrystalline cellulose has been successfully extracted from both walnut shells and apricot shells. Microcrystalline cellulose was well incorporated in PLA matrix with different ratios as checked with FT-IR spectroscopy, tensile test, MFI, ATG, DSC, SEM and optical microscopy. The addition of MCC in PLA matrix has an important effect on the rheology and mechanical proprieties of the resulted composites, where tensile test revealed that there is an increase in Young's modulus but only at an optimum value of WC content in PLA. Nevertheless, a proportional relationship between young's module and AC content in PLA composites was recorded. Melt flow index showed an optimum value for 7% of MCC content for both studied cellulose source WC and AC. The water absorption of prepared composites (PLA/WC and PLA/AC) increased with increasing of MMC loading rate. For all prepared PLA composites, the presence of MCC lead to an enhancement in crystallinity ratio and at the same time a decrease in thermal stability. From the soil burial test, PLA/WC composite presented better biodegradability/weight loss than PLA, from another hand AC in PLA composite don't show a significant effect on weight loss after 12 months of burial.

Finally, the presence of MCC extracted from walnut shells in PLA matrix at 7% of content exhibited the best mechanical properties, crystalline structure and biodegradability rate. Prepared composites can be used as raw materials in industry for manufacturing of medical tool, food packaging, disposable goblets, plates, forks, spoons and food trays.

Data availability statement

The original contributions presented in the study are included in the article/supplementary material, further inquiries can be directed to the corresponding author.

Author contributions

All authors listed have made a substantial, direct, and intellectual contribution to the work and approved it for publication.

Funding

This work was supported by DGRSDT (Direction Générale de la Recherche Scientifique et du Développement Technologique, Algeria).

Conflict of interest

The authors declare that the research was conducted in the absence of any commercial or financial relationships that could be construed as a potential conflict of interest.

Publisher's note

All claims expressed in this article are solely those of the authors and do not necessarily represent those of their affiliated organizations, or those of the publisher, the editors and the reviewers. Any product that may be evaluated in this article, or claim that may be made by its manufacturer, is not guaranteed or endorsed by the publisher.

References

Acquavia, M. A., Pascale, R., Martelli, G., Bondoni, M., and Bianco, G. (2021). Natural polymeric materials : A solution to plastic pollution from the agro-food sector. *Polym. (Basel)* 13, 158. doi:10.3390/polym13010158

Alimuzzaman, S., Gong, R. H., and Akonda, M. (2014). Three-dimensional nonwoven flax fiber reinforced polylactic acid biocomposites. *Polym. Compos.* 35, 1244–1252. doi:10.1002/pc.22774

Arjmandi, R., Hassan, A., Majeed, K., and Zakaria, Z. (2015). Rice husk filled polymer composites. *Int. J. Polym. Sci.* 2015, 1–32. doi:10.1155/2015/501471

Arteaga-Ballesteros, B. E., Guevara-Morales, A., Martín-Martínez, E. S., Figueroa-López, U., and Vieyra, H. (2021). Composite of polylactic acid and microcellulose from kombucha membranes. *e-Polymers* 21, 015–026. doi:10.1515/epoly-2021-0001

Baimark, Y., and Srihanam, P. (2015). Influence of chain extender on thermal properties and melt flow index of stereocomplex PLA. *Polym. Test.* 45, 52–57. doi:10.1016/j.polymertesting.2015.04.017

Barczewski, M., and Mysiukiewicz, O. (2018). Rheological and processing properties of Poly (lactic acid) composites filled with ground chestnut shell. *pk.* 42, 267–274. doi:10.7317/pk.2018.42.2.267

Batakliev, T., Petrova-doycheva, I., Angelov, V., Georgiev, V., Ivanov, E., Kotsilkova, R., et al. (2019). Effects of graphene nanoplatelets and multiwall carbon nanotubes on the structure and mechanical properties of poly (lactic acid) composites : A comparative study. *Appl. Sci. (Basel).* 9, 469. doi:10.3390/app9030469

Bouti, M., Irinislimane, R., and Bensemra, N. B. (2022). Properties investigation of epoxidized sunflower oil as bioplasticizer for Poly (Lactic Acid). *J. Polym. Environ.* 30, 232–245. doi:10.1007/s10924-021-02194-3

Chen, W., Yu, H., Liu, Y., Hai, Y., Zhang, M., and Chen, P. (2011). Isolation and characterization of cellulose nanofibers from four plant cellulose fibers using a chemical-ultrasonic process. *Cellulose* 18, 433–442. doi:10.1007/s10570-011-9497-z

Cinar, S. O., Chong, Z. K., Kucuker, M. A., Wieczorek, N., Cengiz, U., and Kuchta, K. (2020). Bioplastic production from microalgae : A review. *Int. J. Environ. Res. Public Health* 17, 3842. doi:10.3390/ijerph17113842

Costa, L. A. S., Assis, D. D. J., Gomes, G. V. P., da silva, J. B. A., Fonsêca, A. F., and Druzian, J. I. (2015). Extraction and characterization of nanocellulose from corn stover. *Mater. Today Proc.* 2, 287–294. doi:10.1016/j.matpr.2015.04.045

Dogu, B., and Kaynak, C. (2016). Behavior of polylactide/microcrystalline cellulose biocomposites : Effects of filler content and interfacial compatibilization. *Cellulose* 23, 611–622. doi:10.1007/s10570-015-0839-0

Dong, Y., Ghataura, A., Takagi, H., Haroosh, H. J., Nakagaito, A. N., and Lau, K. (2014). Polylactic acid (PLA) biocomposites reinforced with coir fibres : Evaluation of mechanical performance and multifunctional properties. *Compos. Part A Appl. Sci. Manuf.* 63, 76–84. doi:10.1016/j.compositesa.2014.04.003

Dris, R., Gasperi, J., Saad, M., Mirande, C., and Tassin, B. (2016). Synthetic fibers in atmospheric fallout: A source of microplastics in the environment? *Mar. Pollut. Bull.* 104, 290–293. doi:10.1016/j.marpolbul.2016.01.006

Drumright, B. R. E., Gruber, P. R., and Henton, D. E. (2000). Polylactic acid technology. *Adv. Mat.* 12, 1841–1846. doi:10.1002/1521-4095(200012)12:23<1841::aid-adma1841>3.0.co;2-e

El Achaby, M., Kassab, Z., Barakat, A., and Aboulkas, A. (2018). Alfa fibers as viable sustainable source for cellulose nanocrystals extraction : Application for improving the tensile properties of biopolymer nanocomposite films. *Ind. Crops Prod.* 112, 499–510. doi:10.1016/j.indcrop.2017.12.049

Eriksen, M., Lebreton, L. C. M., Carson, H. S., Thiel, M., Moore, C. J., Borerro, J. C., et al. (2014). Plastic pollution in the world's oceans: More than 5 trillion plastic pieces weighing over 250, 000 tons afloat at sea. *PLoS One* 9, e111913–15. doi:10.1371/journal.pone.0111913

Fortunati, E., Armentano, I., Iannoni, A., and Kenny, J. M. (2010). Development and thermal behaviour of ternary PLA matrix composites. *Polym. Degrad. Stab.* 95, 2200–2206. doi:10.1016/j.polymdegradstab.2010.02.034

Frone, A. N., Berlioz, S., Chailan, J. F., and Panaitescu, D. M. (2013). Morphology and thermal properties of PLA-cellulose nanofibers composites. *Carbohydr. Polym.* 91, 377–384. doi:10.1016/j.carbpol.2012.08.054

Gazzotti, S., Rampazzo, R., Hakkarainen, M., Bussini, D., Aldo, M., Farina, H., et al. (2019). Cellulose nano fibrils as reinforcing agents for PLA-based nanocomposites : An *in situ* approach. *Compos. Sci. Technol.* 171, 94–102. doi:10.1016/j.compscitech.2018.12.015

Haafiz, M. K. M., Hassan, A., Zakaria, Z., Inuwa, I. M., Islam, M. S., and Jawaid, M. (2013). Properties of polylactic acid composites reinforced with oil palm biomass microcrystalline cellulose. *Carbohydr. Polym.* 98, 139–145. doi:10.1016/j.carbpol.2013.05.069

Hafizi, W., Ishak, W., Rosli, N. A., and Ahmad, I. (2020). Influence of amorphous cellulose on mechanical , thermal , and hydrolytic degradation of poly (lactic acid) biocomposites. *Sci. Rep.* 1, 11342. doi:10.1038/s41598-020-68274-x

Harini, K., and Chandra Mohan, C. (2020). Isolation and characterization of micro and nanocrystalline cellulose fibers from the walnut shell, corncob and sugarcane bagasse. *Int. J. Biol. Macromol.* 163, 1375–1383. doi:10.1016/j.ijbiomac.2020.07.239

Heidarian, P., Behzad, T., and Sadeghi, M. (2017). Investigation of cross-linked PVA/starch biocomposites reinforced by cellulose nanofibrils isolated from aspen wood sawdust. *Cellulose* 24, 3323–3339. doi:10.1007/s10570-017-1336-4

Hemmati, F., Jafari, S. M., Kashaninejad, M., and Barani Motlagh, M. (2018). Synthesis and characterization of cellulose nanocrystals derived from walnut shell agricultural residues. *Int. J. Biol. Macromol.* 120, 1216–1224. doi:10.1016/j.ijbiomac.2018.09.012

Ibrahim, N., Jollands, M., and Parthasarathy, R. (2019). Morphology and mechanical properties of polylactide/montmorillonite composites. *J. Phys. Conf. Ser.* 1349, 012048. doi:10.1088/1742-6596/1349/1/012048

Jambeck, J. R., Geyer, R., Wilcox, C., Siegler, T. R., Perryman, M., Andrady, A., et al. (2015). Plastic waste inputs from land into the ocean. *Science* 347, 768–770. doi:10.1126/science.1260352Available at: http://www.scopus.com/inward/record.url?eid=2-s2.0-84954204572&partnerID=40&md5=28a97ef4a4fdee6db9ef2fe507a1a02a.

Jiang, L., Zhang, J., and Wolcott, M. P. (2007). Comparison of polylactide/nano-sized calcium carbonate and polylactide/montmorillonite composites : Reinforcing effects and toughening mechanisms. *Polymer* 48, 7632–7644. doi:10.1016/j.polymer.2007.11.001

Kaynak, C., and Meyva, Y. (2014). Use of maleic anhydride compatibilization to improve toughness and other properties of polylactide blended with thermoplastic elastomers. *Polym. Adv. Technol.* 25, 1622–1632. doi:10.1002/pat.3415

Keswani, A., Oliver, D. M., Gutierrez, T., and Quilliam, R. S. (2016). Microbial hitchhikers on marine plastic debris: Human exposure risks at bathing waters and beach environments. *Mar. Environ. Res.* 118, 10–19. doi:10.1016/j.marenvres.2016.04.006

Kim, N. K., Lin, R. J. T., and Bhattacharyya, D. (2014). Extruded short wool fibre composites: Mechanical and fire retardant properties. *Compos. Part B Eng.* 67, 472–480. doi:10.1016/j.compositesb.2014.08.002

Kumar, N., Anil, N., Hazarika, D., Bhagabati, P., Kalamdhad, A., and Katiyar, V. (2021). Biodegradation and characterization study of compostable PLA bioplastic containing algae biomass as potential degradation accelerator. *Environ. Challenges* 3, 100067. doi:10.1016/j.envc.2021.100067

Lee, B., Kim, H., Lee, S., Kim, H., and Dorgan, J. R. (2009). Bio-composites of kenaf fibers in polylactide : Role of improved interfacial adhesion in the carding process. *Compos. Sci. Technol.* 69, 2573–2579. doi:10.1016/j.compscitech.2009.07.015

Lee, C. H., Sapuan, S. M., Lee, J. H., and Hassan, M. R. (2016). Melt volume flow rate and melt flow rate of kenaf fibre reinforced Floreon/magnesium hydroxide biocomposites. *Springerplus* 1, 1680. doi:10.1186/s40064-016-3044-1

Lu, T., Liu, S., Jiang, M., Xu, X., Wang, Y., Wang, Z., et al. (2014). Effects of modifications of bamboo cellulose fibers on the improved mechanical properties of cellulose reinforced poly (lactic acid) composites. *Compos. Part B Eng.* 62, 191–197. doi:10.1016/j.compositesb.2014.02.030

Lv, S., Zhang, Y., Gu, J., and Tan, H. (2017). Biodegradation behavior and modelling of soil burial effect on degradation rate of PLA blended with starch and wood flour. *Colloids Surfaces B Biointerfaces* 159, 800–808. doi:10.1016/j.colsurfb.2017.08.056

Maaloul, N., Ben Arfi, R., Rendueles, M., Ghorbal, A., and Diaz, M. (2017). Dialysis-free extraction and characterization of cellulose crystals from almond (Prunus dulcis) shells. *J. Mat. Environ. Sci.* 8, 4171–4181.

Mahmoud, Y., Safidine, Z., and Belhaneche-Bensemra, N. (2021). Characterization of microcrystalline cellulose extracted from walnut and apricots shells by alkaline treatment. *J. Serb. Chem. Soc.* 86, 521–532. doi:10.2298/jsc200806011m

Mahmoud, Y., Safidine, Z., and Zeghioud, H. (2018). Elaboration of nanostructured polyurethane foams/OMMT using a twin-screw extruder in counter-rotating mode. *J. Serb. Chem. Soc.* 83, 1363–1378. doi:10.2298/JSC180321076M

Mathew, A. P., Oksman, K., and Sain, M. (2004). Mechanical properties of biodegradable composites from poly lactic acid (PLA) and microcrystalline cellulose (MCC). *J. Appl. Polym. Sci.* 97, 2014–2025. doi:10.1002/app.21779

Mofokeng, P., Luyt, A. S., Tábi, T., and Kovács, J. (2012). Comparison of injection moulded, natural fibre-reinforced composites with PP and PLAasmatrices. *J. Thermoplast. Compos. Mater.* 25, 927–948. doi:10.1177/0892705711423291

Moo-Tun, N. M., Iñiguez-Covarrubias, G., and Valadez-Gonzalez, Y. (2020). Assessing the effect of PLA, cellulose microfibers and CaCO3 on the properties of starch-based foams using a factorial design. *Polym. Test.* 86, 106482. doi:10.1016/j.polymertesting.2020.106482

Moran, J. I., Alvarez, V. A., Cyras, V. P., and Vazquez, A. (2008). Extraction of cellulose and preparation of nanocellulose from sisal fibers. *Cellulose* 15, 149–159. doi:10.1007/s10570-007-9145-9

Nurul, M., and Mariatti, M. (2018). Effect of thermal conductive fillers on the properties of polypropylene composites. *J. Thermoplast. Compos. Mater.* 26, 627–639. doi:10.1177/0892705711427345

Olaiya, N. G., Surya, I., Oke, P. K., Rizal, S., Sadiku, E. R., Ray, S. S., et al. (2019). Properties and characterization of a PLA–chitin–starch biodegradable polymer composite. *Polym. (Basel)* 11, 1656. doi:10.3390/polym11101656

Patel, D. K., Lim, S. D., and Dutta, K.-T. (2019). Nanocellulose-based polymer hybrids and their emerging applications in biomedical engineering and water purification. *RSC Adv.* 9, 19143–19162. doi:10.1039/c9ra03261d

Paul, U. C., Fragouli, D., Bayer, I. S., Zych, A., and Athanassiou, A. (2021). Effect of green plasticizer on the performance of microcrystalline cellulose/polylactic acid biocomposites. *ACS Appl. Polym. Mat.* 3, 3071–3081. doi:10.1021/acsapm.1c00281

Qu, P., Gao, Y., Wu, G. F., and Zhang, L. P. (2010). Nanocomposites of Poly(lactic acid) reinforced with cellulose nanofibrils. *BioResources* 5, 1811–1823.

Ramesh, P., Prasad, B. D., and Narayana, K. L. (2021). Influence of montmorillonite clay content on thermal , mechanical , water absorption and biodegradability properties of treated kenaf fiber/PLA-hybrid biocomposites. *Silicon* 13, 109–118. doi:10.1007/s12633-020-00401-9

Salim, M. S., Ariawan, D., Ahmad Rasyid, M. F., Mat Taib, R., Ahmad Thirmizir, M. Z., and Mohd Ishak, Z. A. (2020). Accelerated weathering and water absorption behavior of kenaf fiber reinforced acrylic based polyester composites. *Front. Mat.* 7, 1–15. doi:10.3389/fmats.2020.00026

Shih, Y.-F., and Huang, C.-C. (2011). Polylactic acid (PLA)/banana fiber (BF) biodegradable green composites. *J. Polym. Res.* 18, 2335–2340. doi:10.1007/s10965-011-9646-y

Silva, D., Kaduri, M., Poley, M., Adir, O., and Krinsky, N. (2020). Europe PMC funders group biocompatibility , biodegradation and excretion of polylactic acid (PLA) in medical implants and theranostic systems. *Chem. Eng. J.* 340, 9–14. doi:10.1016/j.cej.2018.01.010.Biocompatibility

Soleimani, M., Tabil, L. G., Panigrahi, S., and Opoku, A. (2008). The effect of fiber pretreatment and compatibilizer on mechanical and physical properties of flax fiber-polypropylene composites. *J. Polym. Environ.* 16, 74–82. doi:10.1007/s10924-008-0102-y

Sukyai, P., Sriroth, K., Lee, B.-H., and Kim, H.-J. (2012). The effect of bacterial cellulose on the mechanical and thermal expansion properties of kenaf/polylactic acid composites. *Appl. Mech. Mat.* 119, 1343–1351. doi:10.4028/www.scientific.net/amm.117-119.1343

Van Cauwenberghe, L., Devriese, L., Galgani, F., Robbens, J., and Janssen, C. R. (2015). Microplastics in sediments: A review of techniques, occurrence and effects. *Mar. Environ. Res.* 111, 5–17. doi:10.1016/j.marenvres.2015.06.007

Wang, Q., Ji, C., Sun, J., Zhu, Q., and Liu, J. (2020). Structure and properties of polylactic acid biocomposite films reinforced with cellulose nanofibrils. *Molecules* 25, 3306. doi:10.3390/molecules25143306

Yaacob, N. D., Ismail, H., and Ting, S. S. (2016). Soil burial of polylactic acid/paddy straw powder biocomposite. *BioResources* 11, 1255–1269. doi:10.15376/biores.11.1.1255-1269

Yew, G. H., Yusof, A. M. M., Ishak, Z. A. M., and Ishiaku, U. S. (2005). Water absorption and enzymatic degradation of poly (lactic acid)/rice starch composites. *Polym. Degrad. Stab.* 90, 488–500. doi:10.1016/j.polymdegradstab.2005.04.006

Yorseng, K., Rangappa, S. M., Pulikkalparambil, H., Siengchin, S., and Parameswaranpillai, J. (2020). Accelerated weathering studies of kenaf/sisal fiber fabric reinforced fully biobased hybrid bioepoxy composites for semi-structural applications: Morphology, thermo-mechanical, water absorption behavior and surface hydrophobicity. *Constr. Build. Mat.* 235, 117464. doi:10.1016/j.conbuildmat.2019.117464

Yussuf, A. A., Massoumi, I., and Hassan, A. (2010). Comparison of Polylactic Acid/kenaf and Polylactic Acid/rise husk composites : The influence of the natural fibers on the mechanical, thermal and biodegradability properties. *J. Polym. Environ.* 18, 422–429. doi:10.1007/s10924-010-0185-0

Zhang D, D., Liu, X., Huang, W., Li, J., Wang, C., Zhang, D., et al. (2020). Microplastic pollution in deep-sea sediments and organisms of the Western Pacific Ocean. *Environ. Pollut.* 259, 113948. doi:10.1016/j.envpol.2020.113948

Zhang Q, Q., Lei, H., Cai, H., Han, X., Lin, X., Qian, M., et al. (2020). Improvement on the properties of microcrystalline cellulose/polylactic acid composites by using activated biochar. *J. Clean. Prod.* 252, 119898. doi:10.1016/j.jclepro.2019.119898

Zhang, Q., Yi, W., Li, Z., Wang, L., and Cai, H. (2018). Mechanical properties of rice husk biochar reinforced high density polyethylene composites. *Polymers.* 10, 286. doi:10.3390/polym10030286

Zhou, Y., Lei, L., Yang, B., Li, J., and Ren, J. (2018). Preparation and characterization of polylactic acid (PLA) carbon nanotube nanocomposites. *Polym. Test.* 68, 34–38. doi:10.1016/j.polymertesting.2018.03.044

Zou, G. X., Zhang, X., Zhao, C. X., and Li, J. (2012). The crystalline and mechanical properties of PLA/layered silicate degradable composites. *Polym. Sci. Ser. A* 54, 393–400. doi:10.1134/S0965545X12050148